DOI: 10.18721/JPM.12111
УДК 531.391+681.5.01

THE DAMPING OF THE DISTRIBUTED SYSTEM VIBRATIONS USING PIEZOELECTRIC TRANSDUCERS: SIMULATION

A.V. Fedotov

Institute for Problems of Mechanical Engineering, RAS,

St. Petersburg, Russian Federation

The present paper continues the author's studies where the problem of the control of forced bending vibrations of a metal beam using piezoelectric sensors and actuators has been investigated. In those studies, all the control results were obtained experimentally. However, in order to make the design of the control systems the most effective, it was necessary to develop a numerical model, which would allow one to get the results for different variants of such systems, and that was the objective of the present study. In this study, the main experimental data were reproduced numerically on a basis of the finite element model of the object. In addition, new modal control systems were designed, providing a more efficient reduction of the amplitude of resonance vibrations of a beam compared to the systems considered experimentally.

Keywords: active vibration control, mechatronics, modal control, piezoelectric transducer, finite element model

Citation: A.V. Fedotov, The damping of the distributed system vibrations using piezoelectric transducers: simulation, St. Petersburg Polytechnical State University Journal. Physics and Mathematics. 12 (1) (2019) 130–142. DOI: 10.18721/JPM.12111

ЧИСЛЕННОЕ МОДЕЛИРОВАНИЕ ГАШЕНИЯ КОЛЕБАНИЙ РАСПРЕДЕЛЕННОЙ СИСТЕМЫ С ПОМОЩЬЮ ПЬЕЗОЭЛЕМЕНТОВ

А.В. Федотов

Институт проблем машиноведения РАН, Санкт-Петербург, Российская Федерация

Представленная статья продолжает работы автора, в которых рассматривалась задача об управлении вынужденными изгибными колебаниями металлической балки с помощью пьезоэлектрических сенсоров и актуаторов. При этом все результаты управления были получены экспериментально. Однако для того, чтобы процесс проектирования систем управления был наиболее эффективным, необходима разработка численной модели, позволяющей получать результаты для разных вариантов таких систем, что и является задачей данной работы. В данном исследовании численно на основе конечно-элементной модели объекта воспроизводятся основные экспериментальные результаты, а также проектируются более эффективные модальные системы управления, приводящие к большему снижению амплитуды резонансных колебаний балки, по сравнению с системами, рассмотренными ранее в эксперименте.

Ключевые слова: управление колебаниями, мехатроника, модальное управление, пьезоэлемент, конечно-элементная модель

Ссылка при цитировании: Федотов А.В. Численное моделирование гашения колебаний распределенной системы с помощью пьезоэлементов // Научно-технические ведомости СПбГПУ. Физико-математические науки. 2019. Т. 12. № 1. С. 142–155. DOI: 10.18721/JPM.12111

Introduction

Controlling the vibrations in distributed mechanical systems is complicated because these systems have an infinite number of vibration modes, so they are not fully controllable and observable. In practice, however, dynamics of such systems can be usually analyzed by considering some finite set of the object's normal modes. It was experimentally confirmed in [1] for such cases that modal control, specifically of the forms mainly involved in operation of the given system, had a greater efficiency compared with local control.

The modal approach to vibration control in elastic systems was first formulated in [2] and further developed in [3]. Specific vibration modes of an elastic object can be monitored or controlled via distributed sensors and actuators used as modal filters [4, 5] and arrays of discrete control elements [6–8]. The problem of identifying the control object arises in the latter case, typically solved either by finite element modeling of the object [9–11] or analytically [12, 13]. We have proposed an experimental procedure for identifying an object with the purpose of creating a modal control system in [14]. Piezoelectric sensors and actuators are easy to use and have high performance characteristics, making them widely popular for vibration control in distributed systems.

This paper continues the studies in [1, 14], detailing the experiments on creating control systems that reduce forced vibrations of a cantilevered metal beam. The control systems obtained use a set of discrete piezoelectric sensors and actuators. Both local and modal control systems were constructed as part of the experiment; it was the modal system that proved the most effective one.

The goal of this study has consisted in numerically reproducing the main experimental results and in creating control systems that are more efficient compared with those obtained within the framework of previous experiments.

The first section of the study considers an experimental setup for controlling forced bending vibrations of a beam; the results of finite element modeling of the control object are then described and compared with the results of the experiment. Next, we have outlined the theoretical foundations of modal vibration control in distributed mechanical systems, formulating the stability criteria for a closed-loop system with two feedback loops. The paper is concluded by considering the operation of various control systems that reduce the resonant vibration amplitude of a beam.

Experimental setup

The setup, procedure and results of the experimental study considered in this paper are described in detail in [1, 14].

The schematic for the experimental setup is shown in Fig. 1, *a*. A 70 cm long aluminum beam *1* with a rectangular cross-section of 3 Ч 35 mm, disposed vertically and fixed at one point at a distance of 10 cm from the lower end, was chosen as the control object. This beam experiences forced bending vibrations induced by longitudinal vibration of piezoelectric stack actuator *2*, which is part of the structure connecting the beam to fixed base *3*.

The main purpose of the experimental setup constructed was to perfect the modal approach to control of forced beam vibrations. In order to do this, we designed a control system with two loops including two actuators and two sensors. Piezoelectric actuators *4* and sensors *5* are arranged in pairs on both sides of the beam. Fig. 1, *b* shows a fragment of a finite element model of the beam comprising the fixed stack *2* and one of actuators *4*. In contrast to the simplified scheme given in Fig. 1, *a*, the finite element model includes a complete structure for the beam's fixation used in the experimental setup. The structure includes (in addition to the piezoelectric stack actuator) a steel plate and studs receiving the weight of the beam and thus taking the lateral load off the actuator.

The signals measured by the sensors are converted via discrete controller *6* into control signals supplied to the actuators. The task of the control system is to reduce the amplitude of forced resonant vibrations of the beam with the first and second natural frequencies. Modal control is thus carried out for the first and second modes of the beam's bending vibrations. These modes are shown in Fig. 1, *c*. The quality of suppression of forced vibrations is assessed from the readings of a laser vibrometer measuring the vibration velocity of the beam's upper endpoint. This point has the highest vibration amplitude of all points of the beam for both the first and second modes.

Actuators and sensors are identical rectangular 50 × 30 × 0.5 mm plates made of piezoelectric material, covered with electrodes on both sides and placed inside thin insulation. These piezoelectric elements were considered in [15]. When electric voltage is applied to the actuator electrodes, the piezoelectric layer is either stretched or compressed, resulting in bending deformation of the segment of the beam to which the actuator is glued. Thus, the

impact of the actuator on the beam is equivalent to applying a pair of opposite bending moments to two cross-sections of the beam (end sections of the actuator). The piezoelectric sensor operates by similar principles: as a segment of the beam to which the sensor is attached bends, the sensor material is either stretched or compressed in the longitudinal direction, resulting in potential difference measured as a signal from the sensor appearing on the sensor electrodes. To achieve maximum efficiency in controlling the first and second modes of the beam's bending vibrations, sensors and actuators are located in the points of the beam where these modes have the greatest curvature:

$$110.5 \le x \le 160.5 \text{ mm}$$

for the first sensor/actuator pair and

$$377.5 \le x \le 427.5 \text{ mm}$$

for the second pair (the x coordinate is measured from the lower end of the beam).

In addition to the main elements (see Fig. 1), the control system additionally includes:

an amplifier increasing the amplitude of the control signal by 25 times before it is fed to the actuators;

low-pass filters with a cut-off frequency of 1 kHz smoothing the high-frequency component of the electrical signal and protecting the equipment from high input voltages.

Both the measured signal before it is fed to the controller and the control signal before it is fed to the actuators pass through the filter.

A number of characteristics of the control object should be measured in order to design a control system.

Firstly, we measured the frequency and phase response of the beam upon impact on each of the actuators and as the signal was measured by each sensor.

Secondly, the frequency response and the phase response of the beam were also read upon impact on the stack actuator and as the signal was measured with the vibrometer. Thus, we obtained a total of 9 frequency and phase response curves for each of the 3 cases for external impacts (actuators, piezoelectric stack) and each of the 3 cases for measurements (sensors, vibrometer). All characteristics were measured with filters and amplifiers present.

Thirdly, we analyzed the beam's vibrations in resonant modes (resonant vibrations with the first and second natural frequencies) in order to determine the modal matrices T and F, in accordance with the identification procedure described in [14].

After that, based on the measured characteristics

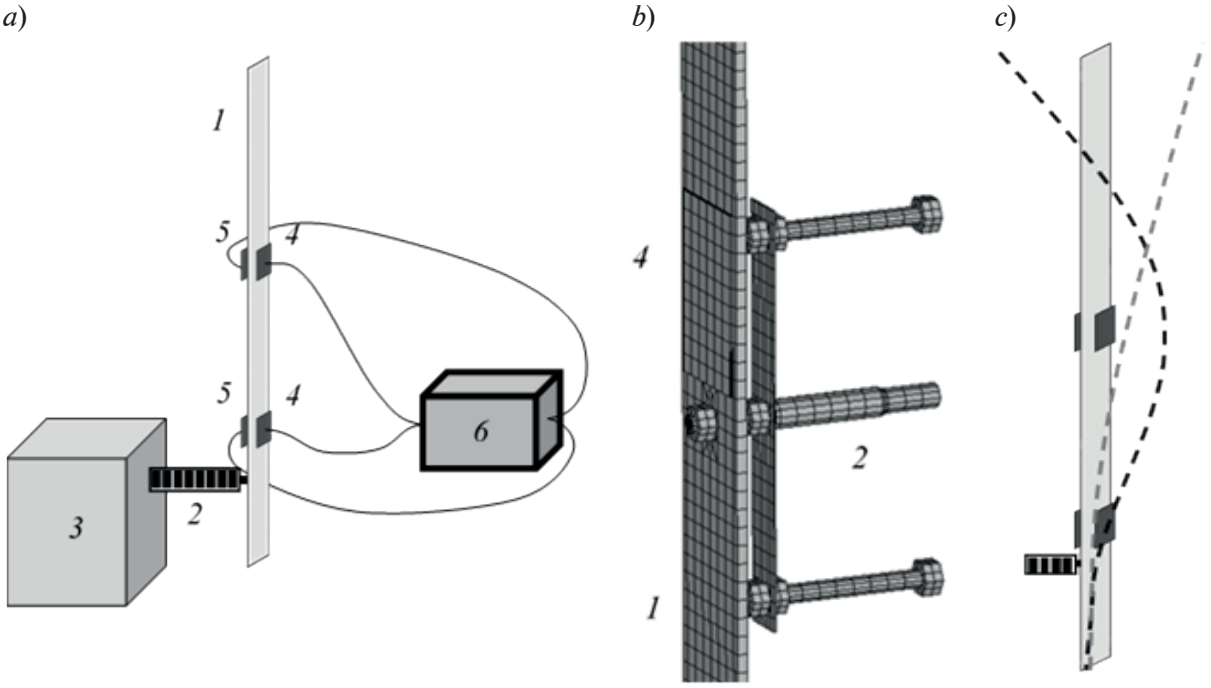

Fig. 1. Schematic of experimental setup (*a*), fragment of finite element model of object (*b*) and two lowest bending vibration modes of beam (*c*)
aluminum beam *1*; piezoelectric stack *2*; fixed base *3*;
actuators *4*; sensors *5*; controller *6*

of the object, we used the method of logarithmic amplitude-frequency characteristics to formulate and then experimentally test the control laws providing the most effective suppression of the beam's forced resonant vibrations.

As a result, we obtained local control systems and a modal control system.

It was the modal system that proved the most effective, allowing to reduce the resonant vibration amplitudes by 83.5% at the first resonance, and by 87.2% at the second. The local control systems we designed yielded good results either at the first (decrease by 78.0%) or at the second (decrease by 88.9%) resonance but it was impossible to obtain a control system that would be simultaneously and equally effective at both resonances within the local approach. The test results for the obtained control systems are described in detail in [1].

Finite-element model of the system

One of the goals of our study was to numerically reproduce the results obtained in the experiment described in the previous section of the paper. For this purpose, we simulated the given system in the ANSYS finite element (FE) package. A fragment of the FE model of the beam with piezoelectric sensors and actuators is shown in Fig. 1, *b*.

The FE model consists of three-dimensional 20-node elements Solid186 (used for common materials: aluminum of the beam, steel of the support structures and insulation of piezoelectric elements) and Solid226 (for piezoelectric materials of sensors, actuators and stacks). The model contains the total of 3534 elements and 21088 nodes. Rigid clamping was given as the mechanical boundary conditions for the points of the support structure which were attached to the fixed base in the experimental setup; electric potentials on the actuator and stack electrodes were given as electrical boundary conditions.

To set the damping factor, we analyzed the experimental results in the CE model of the experimental setup, determining the damping factor ξ from the width of the resonant peak in each of the resonances for all frequency response curves, in accordance with the formula

$$\xi = \frac{\Delta f}{2 f_0}, \qquad (1)$$

where f_0 is the resonant frequency; Δf is the width of the resonant peak, bounded by the frequency values at which the resonant amplitude falls by $\sqrt{2}$ times.

The values of the damping factors obtained this way are given in Table 1 (see the note to Table 1 for notations). As a result, the same damping factor $\xi = 0.0020$ was set for all vibration modes in the FE model.

Harmonic analysis of the system was

Table 1

Damping factors obtained from experimental frequency response at different resonant frequencies f_0

Mode number	f_0, Hz	ξ_1	ξ_2	ξ_3	ξ_4
1	7.125	0.0044	0.0044	0.0055	0.0055
2	42.55	0.0022	0.0021	0.0026	0.0026
3	113.9	0.0031	0.0031	0.0034	0.0034
4	175.2	0.0022	0.0025	0.0031	0.0031
5	249.5	0.0018	0.0019	0.0019	0.0019
6	390.9	0.0010	0.0010	0.0012	0.0010
7	579.4	0.0013	0.0012	0.0016	0.0016
8	790.5	0.0010	0.0009	0.0014	0.0014
9	1073	0.0016	0.0016	0.0018	0.0017
10	1338	0.0015	0.0014	0.0019	0.0019
11	1471	0.0016	0.0017	0.0025	0.0025
12	1763	0.0022	0.0023	0.0034	0.0033

Notations: ξ_1–ξ_4 are the damping factors obtained for different frequency responses: actuator-sensor (ξ_1), actuator-vibrometer (ξ_2), stack-sensor (ξ_3), stack-vibrometer (ξ_4)

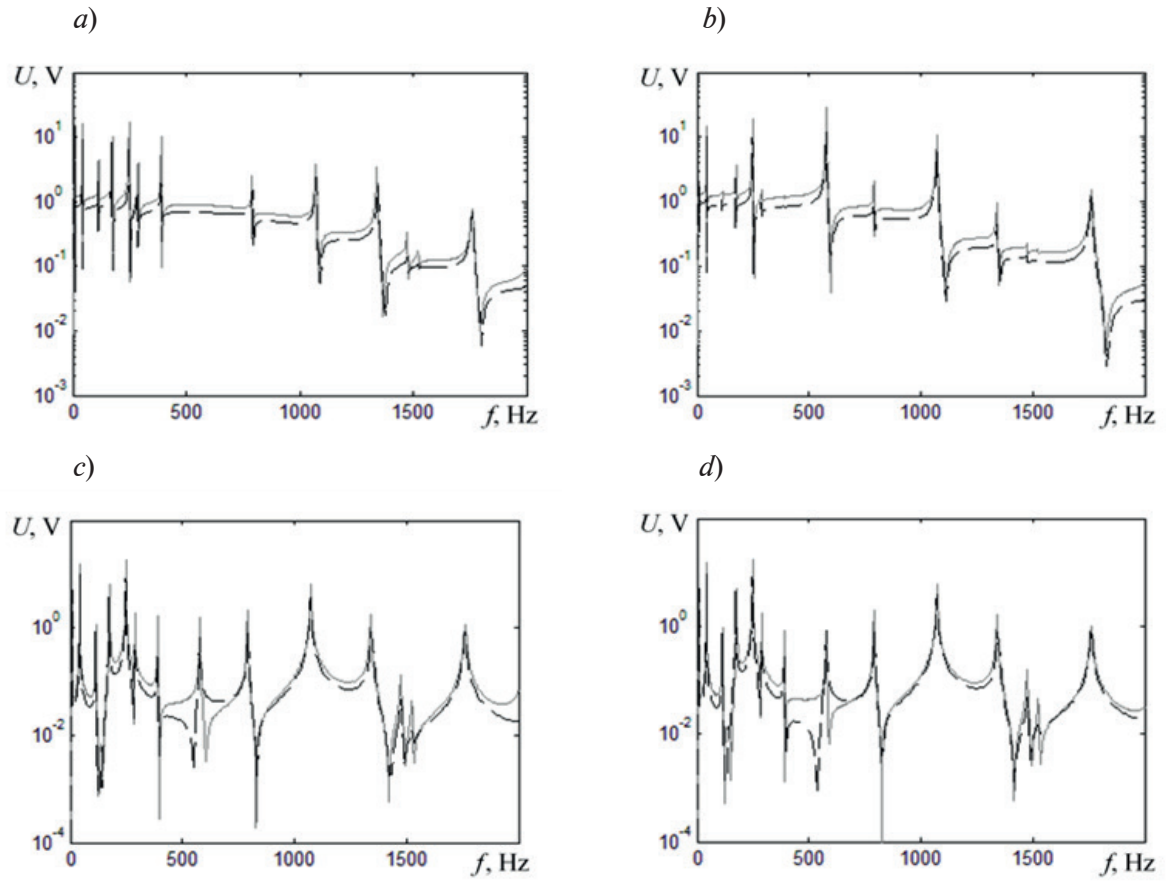

Fig. 2. Comparison of frequency response obtained experimentally (solid lines) and numerically (dashed lines) for impact on actuators *A*1 (*a*, *c*), *A*2 (*b*, *d*) and measurement of signals from sensors *S*1 (*a*, *d*) and *S*2 (*b*, *c*)

performed in the ANSYS package with three variants of action: using each of the two actuators or the piezoelectric stack. Three frequency responses and phase responses were recorded for each variant, corresponding to either signal measurement by one of two sensors, or to transverse displacement of a point at the upper end of the beam. After these characteristics were obtained in ANSYS, they were modified: the characteristics of filters and amplifiers, measured separately as part of the experiment, were added. Thus, the frequency and phase response curves similar to those measured experimentally were obtained.

A comparison of the frequency response obtained numerically and experimentally for each of the two actuators and each of the two sensors is given in Fig. 2. It can be seen that the resonant frequencies in the experiment and in the FE model are in good agreement, but the amplitudes of the experimental curves turn out to be slightly higher than of those obtained by simulation. There is additional disagreement in the magnitudes of the resonant peaks of the curves, since damping is in fact different for different forms of vibrations and differs from the value chosen in the model. However, in general, the data obtained numerically agree well with the experimental results.

Modal control of vibrations in elastic system

Let us consider the operation of a modal system for controlling vibrations in an elastic object, consisting of n sensors and n actuators. The main principle of modal control is that different vibration modes are controlled separately; at the same time, each control loop corresponds to its own vibration mode. Let the control system contain m loops, and control be carried out for m lower vibration modes. It is evident that the number of sensors and actuators used should be no less than the number of independently controlled forms, i.e. $n \geq m$.

Let us assume that the dynamics of a distributed system can be described by using

an expansion of the displacement $u(r,t)$ in terms of the system's normal vibration modes:

$$u(r,t) = \sum_{k=1}^{\infty} w_k(r)\beta_k(t), \qquad (2)$$

where $\beta_k(t)$ are the generalized coordinates, $w_k(r)$ are the vibration modes.

Let the vibration modes be independent of each other; the dynamics of each of the modes is then described by the equation

$$\ddot{\beta}_k(t) + 2\xi_k\lambda_k\dot{\beta}_k(t) + \lambda_k^2\beta_k(t) = f_k + y_k, \qquad (3)$$

where λ_k is the kth normal frequency of the object; ξ_k is the kth damping factor; f_k is the kth generalized external force; y_k is the control action corresponding to the kth mode of the object's vibrations.

The control action is applied to the object using n actuators and is a linear combination of control signals U_i fed to the actuators for each vibration mode:

$$y_k = \sum_{i=1}^{n} \theta_{ki}^a U_i, \qquad (4)$$

where θ_{ki}^a is the coefficient for the impact of an ith actuator on a kth vibration mode.

Separation of the object's first m vibration modes in the control system is provided by the following control structure:

$$U_{n\times 1} = FK_{m\times m}TY_{n\times 1}, \qquad (5)$$

where $K_{m\times m}$ is the diagonal matrix of control laws where each element K_{ii} corresponds to one of the control loops and is a function of the complex variable s; $F_{n\times m}$, $T_{m\times n}$ are modal matrices (synthesizer and analyzer) that perform linear transformation of the vectors of control and measured signals; $Y_{n\times 1}$ is the vector of sensor signals.

The vector $Y_{n\times 1}$ is related to the vector of the first m generalized coordinates $\beta_{m\times 1}$ as follows:

$$Y_{n\times 1} = \theta^s_{n\times m}\beta_{m\times 1} + \tilde{Y}, \qquad (6)$$

where $\theta^s_{n\times m}$ is the weight matrix determining how each of the n sensors reacts to each of the m vibration modes; $\tilde{Y}$ is the term dependent only on the object's higher normal modes which are not controlled.

Substituting expressions (4)–(6) into Eq. (3), we obtain the equation of motion for m first generalized coordinates in the matrix form:

$$\begin{gathered}\ddot{\beta}_{m\times 1} + 2\xi_{m\times m}\Lambda_{m\times m}\dot{\beta}_{m\times 1} + \\ +\Lambda^2_{m\times m}\beta_{m\times 1} = \\ = f_{m\times 1} + \theta^a{}_{m\times n}F_{n\times m}K_{m\times m}\times \\ \times T_{m\times n}\theta^s{}_{n\times m}\beta_{m\times 1} + \Delta_{m\times 1},\end{gathered} \qquad (7)$$

where $\Lambda_{m\times m}$, $\xi_{m\times m}$ are diagonal matrices of natural frequencies and damping factors, respectively; $\Delta_{m\times 1}$ is a vector containing only higher harmonics.

Clearly, for separate control of the object's m lower vibration modes, the diagonal structure of the matrix

$$M = \theta^a FKT\theta^s$$

has to be obtained.

For this purpose, the modal matrices F and T should be defined as follows:

$$\begin{aligned} T_{m\times n} &= (\theta^{sT}_{m\times n}\theta^s_{n\times m})^{-1}\theta^{sT}_{m\times n}, \\ F_{n\times m} &= \theta^{aT}_{n\times m}(\theta^a_{m\times n}\theta^{aT}_{n\times m})^{-1}. \end{aligned} \qquad (8)$$

Thus, the modal matrices F and T should be given first in accordance with formula (8), and the control laws should be chosen next for each loop $K_{ii}(s)$ in order to create a modal control system.

Stability of closed system with two feedback loops

First of all, let us consider the operation of a control system with one feedback loop. Let the disturbance d be fed to the input of the control object with the transfer function $H(s)$, with the object's output signal y converted to the control action u in the feedback loop with the transfer function $R(s)$, which is also fed to the object's input with a minus sign. Thus, the output and control signals are related by the following expressions:

$$\begin{aligned} y &= H(s)\,(d-u), \\ u &= R(s)\,y. \end{aligned} \qquad (9)$$

Let us confine ourselves to considering the transfer functions $H(s)$ and $R(s)$ which do not have poles in the right complex half-plane of the variable s. Thus, the open-loop system is stable. The relationship between the input and output signals of the system is derived from relations (9):

$$y = \frac{H(s)}{1+H(s)R(s)}d = \frac{H(s)}{1+H_0(s)}d. \qquad (10)$$

In order to determine the stability of a closed-loop system, we should analyze the function in the denominator of the obtained fraction. For a closed-loop system to be stable, all zeros of this function should lie in the left half-plane of s. However, in practice it is more convenient to confine the consideration with analysis of the transfer function of an open-loop system

$$H_0(s) = H(s)R(s).$$

According to the Nyquist criterion, provided that an open-loop system is stable, a

closed-loop system is stable if the hodograph of the function $H_0(i\omega)$ does not enclose the point (−1; 0) on the complex plane as the frequency ω changes from 0 to +∞. Now let us obtain a similar criterion for a system with two feedback loops.

Let the control object have two inputs and two outputs, with disturbances d_1 and d_2 fed to the inputs, and the output signals y_1 and y_2 measured by the control system and converted by the transfer functions $R_1(s)$ and $R_2(s)$ to control actions u_1 and u_2, also fed with a minus sign to the object's inputs:

$$\begin{aligned} u_1 &= R_1(s)\, y_1, \\ u_2 &= R_2(s)\, y_2. \end{aligned} \tag{11}$$

To describe the behavior of the object in the given system, we use four transfer functions, $H_{11}(s)$, $H_{12}(s)$, $H_{21}(s)$ and $H_{22}(s)$, each of them corresponding to one of the two inputs and one of the two outputs:

$$\begin{aligned} y_1 &= H_{11}(s)(d_1-u_1)+H_{21}(s)(d_2-u_2), \\ y_2 &= H_{12}(s)(d_1-u_1)+H_{22}(s)(d_2-u_2) \end{aligned} \tag{12}$$

Here we also assume that all transfer functions $H_{ij}(s)$ and $R_i(s)$ do not have poles in the right half-plane of s. The expressions relating input and output signals of the system with closed control loops are obtained from equalities (11) and (12) by simple mathematical transformations:

$$\begin{aligned} y_1 = \Big(\big(H_{11}(s)+\big(H_{11}(s)H_{22}(s)- \\ -H_{12}(s)H_{21}(s)\big)R_2(s)\big)d_1+ \\ +H_{21}(s)d_2\Big)\Big/\Big(\big(1+H_{11}(s)R_1(s)\big)\times \\ \times\big(1+H_{22}(s)R_2(s)\big)- \\ -H_{12}(s)H_{21}(s)R_1(s)R_2(s); \end{aligned} \tag{13}$$

$$\begin{aligned} y_2 = \Big(\big(H_{22}(s)+\big(H_{11}(s)H_{22}(s)- \\ -H_{12}(s)H_{21}(s)\big)R_1(s)\big)d_2+ \\ +H_{12}(s)d_1\Big)\Big/\Big(\big(1+H_{11}(s)R_1(s)\big)\times \\ \times\big(1+H_{22}(s)R_2(s)\big)- \\ -H_{12}(s)H_{21}(s)R_1(s)R_2(s). \end{aligned} \tag{14}$$

The denominator of the obtained fractions (the same for both of them) is analyzed to determine the stability of the system. Notably, this function has no poles in the right half-plane of s. Therefore, the same as in the case of system with one loop, the closed-loop system is stable if all zeros of this function lie in the left complex half-plane of the variable s.

The denominator of fractions (13) and (14) may be rewritten as

$$1 + H_0(s),$$

where the function $H_0(s)$ is defined as follows:

$$\begin{aligned} H_0(s) = H_{11}(s)R_1(s)+ \\ +H_{22}(s)R_2(s)+ \\ +\big(H_{11}(s)H_{22}(s)- \\ -H_{12}(s)H_{21}(s)\big)R_1(s)R_2(s). \end{aligned} \tag{15}$$

Therefore, a criterion similar to the Nyquist criterion can be applied for the given system: for this system to be stable, the hodograph of the function $H_0(i\omega)$ should not enclose the point (−1; 0) on the complex half-plane as the frequency ω changes from 0 to +∞.

Construction of control systems

The first step in constructing a modal control system is defining the modal matrices F (synthesizer) and T (analyzer). The corresponding experimental procedure including studies of resonant modes is given in [14].

The heights of the first and second resonant peaks on the stack-sensor and actuator-vibrometer frequency response curves are analyzed to calculate the modal matrices for numerical solution of the problem. The modal synthesizer F is set so that the first control loop does not induce vibrations of the second mode in the beam and the second loop so that it does not induce vibrations of the first mode. Similarly, the modal analyzer T is set so that the first loop does not react to activation of the second vibration mode, and the second so that it does not react to activation of the first mode.

Analysis of the frequency response revealed that the first and second actuators excite the first mode of the beam's bending vibrations in a ratio of 3.08 : 1.00 and the second form in a ratio of −0.97 : 1.00. The first and second sensors respond to activation of the first mode in a ratio of 3.07 : 1.00, and of the second in a ratio of −0.95 : 1.00. Modal matrices were then obtained from here:

$$\begin{aligned} F &= \begin{bmatrix} 1.01 & -0.49 \\ 0.98 & 1.50 \end{bmatrix}, \\ T &= \begin{bmatrix} 1.01 & 0.96 \\ -0.49 & 1.49 \end{bmatrix}. \end{aligned} \tag{16}$$

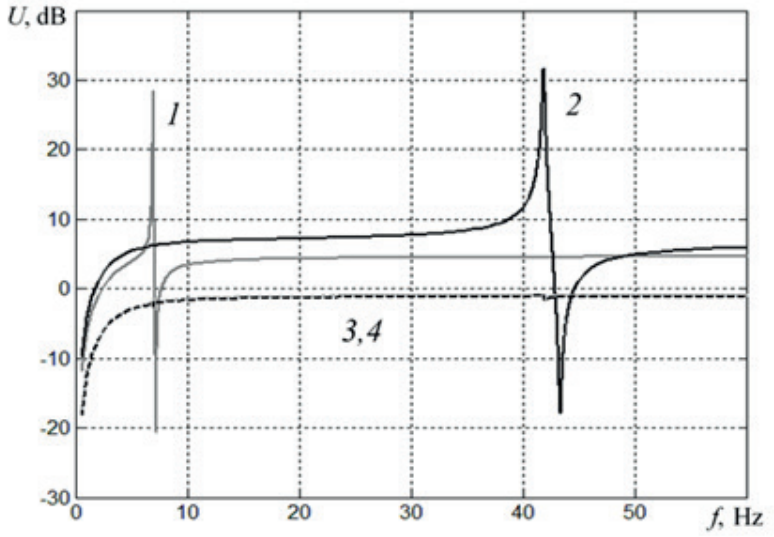

Fig. 3. Frequency response for system corresponding to excitation of vibrations with *i*th modal control loop and measurement with *j*th modal loop; ij = 11 (curve *1*), 22 (*2*), 12 (*3*) and 21 (*4*)

These values are sufficiently close to the values of the matrices obtained in the experiment:

$$F^{(\exp)} = \begin{bmatrix} 1.000 & -0.500 \\ 1.035 & 1.525 \end{bmatrix}, \quad T^{(\exp)} = \begin{bmatrix} 1.00 & 1.01 \\ -0.49 & 1.52 \end{bmatrix}. \tag{17}$$

The results of mode separation in modal control loops using the T and F matrices are shown in Fig. 3. The figure also shows the absolute values of the transfer functions H^m_{ij}, corresponding to excitation of vibrations with the *i*th modal control loop and measurement with the *j*th modal loop. These functions are obtained from the transfer functions H_{ij} corresponding to excitation of vibrations with the *i*th actuator and to measurement with the *j*th sensor according to the following formula:

$$H^m_{ij} = \sum_{k=1}^{2}\sum_{l=1}^{2} T_{jl} F_{ki} H_{kl}. \tag{18}$$

As can be seen from the figure, the selected modal matrices provide a good quality of separation of the first and second vibration modes: only the first resonant peak is present on the frequency response curve for H^m_{11} corresponding to the first modal control loop; only the second resonance peak on the frequency response curve for H^m_{22}, with both resonances missing on the cross-coupled frequency response curves for H^m_{12} and H^m_{21}. This means that mutual influence of the control loops is minimal.

Numerical study of the beam's vibrations with control should involve both constructing the control systems and obtaining the results using these systems. The control systems are used to analyze the frequency response curves of the beam, obtained by excitation of vibrations with the stack and by measurement of the vibration amplitude of a point at the upper end of the beam. The effectiveness of the constructed control systems is assessed by comparing the frequency response data near the first and second resonant frequencies of the beam's bending vibrations with the control system turned on and off. The frequency response of the beam with control is obtained from the existing frequency and phase responses of the beam without control in accordance with the mathematical procedure outlined below.

Let three sources of excitation act on the beam, namely, the voltages:

U_d supplied to the stack;

U_1 supplied to the first actuator;

U_2 supplied to the second actuator.

In this case, the transverse displacement y of the point at the upper end of the beam, the voltage Y_1 in the first sensor and Y_2 in the second sensor are measured. The measured values are expressed in terms of the applied

impacts using transfer functions H_d, $H^{(1)}{}_d$, $H^{(2)}{}_d$, $H^{(1)}{}_a$, $H^{(2)}{}_a$, $H^{(11)}{}_{as}$, $H^{(12)}{}_{as}$, $H^{(21)}{}_{as}$, $H^{(22)}{}_{as}$:

$$\begin{cases} y = H_d U_d + H_a^{(1)} U_1 + H_a^{(2)} U_2, \\ Y_1 = H_d^{(1)} U_d + H_{as}^{(11)} U_1 + H_{as}^{(21)} U_2, \\ Y_2 = H_d^{(2)} U_d + H_{as}^{(12)} U_1 + H_{as}^{(22)} U_2. \end{cases} \quad (19)$$

Let the control actions U_1 and U_2 depend on the measured signals Y_1 and $Y_{2\text{ of the}}$ sensors in the following way:

$$\begin{cases} U_1 = -R_{11} Y_1 - R_{12} Y_2, \\ U_2 = -R_{21} Y_1 - R_{22} Y_2. \end{cases} \quad (20)$$

In this case, we can express the displacement y of the point at the upper end of the beam in terms of the voltage U_d applied to the stack by simple mathematical transformations:

$$\begin{cases} y = H_d U_d + H_a^{(1)} U_1 + H_a^{(2)} U_2, \\ U_1 = U_d \left(-R_{21} H_d^{(1)} - R_{22} H_d^{(2)} + \right. \\ + \left(R_{11} R_{22} - R_{12} R_{21} \right) \times \\ \left. \times \left(H_{as}^{(12)} H_d^{(1)} - H_{as}^{(11)} H_d^{(2)} \right) \right) \Big/ \left(1 + \right. \\ + R_{11} H_{as}^{(11)} + R_{12} H_{as}^{(12)} + R_{21} H_{as}^{(21)} + \\ + R_{22} H_{as}^{(22)} + \left(R_{11} R_{22} - R_{12} R_{21} \right) \times \\ \left. \times \left(H_{as}^{(11)} H_{as}^{(22)} - H_{as}^{(12)} H_{as}^{(21)} \right) \right), \\ U_2 = U_d \left(-R_{11} H_d^{(1)} - R_{12} H_d^{(2)} - \right. \\ - \left(R_{11} R_{22} - R_{12} R_{21} \right) \times \\ \left. \times \left(H_{as}^{(22)} H_d^{(1)} - H_{as}^{(21)} H_d^{(2)} \right) \right) \Big/ \left(1 + \right. \\ + R_{11} H_{as}^{(11)} + R_{12} H_{as}^{(12)} + \\ + R_{21} H_{as}^{(21)} + R_{22} H_{as}^{(22)} + \\ + \left(R_{11} R_{22} - R_{12} R_{21} \right) \times \\ \left. \times \left(H_{as}^{(11)} H_{as}^{(22)} - H_{as}^{(12)} H_{as}^{(21)} \right) \right). \end{cases}$$

Thus, based on the known transfer functions of the system without control and the selected control laws, we have calculated the transfer functions of the control system.

Within the framework of this numerical study, we first tested modal control system I, assembled experimentally. Next, we constructed modal control system II, differing from system I by the transfer functions in control loops. The goal in constructing system II was to obtain a control system that would most effectively reduce the amplitude of forced bending vibrations of the beam at the first and second resonances. System I, tested in numerical study, differs from the modal system used in the experiment only by the gains in control loops, which were selected from the condition of the greatest efficiency of the system.

The transfer functions and gains for both loops of control systems I and II are given in Appendix.

Fig. 4, *a* shows the Nyquist diagram for control system I, obtained for both control loops in accordance with formula (15). Fig. 4, *b* shows a segment of this diagram near the point (−1; 0). Since the hodograph does not enclose the point (−1; 0) on the complex plane, this control system is stable. The Nyquist diagram for control system II looks similar.

Fig. 5 shows the frequency response curve of the beam, obtained for impact with the stack and measurement of the vibration amplitude of the point at the upper end of the beam with and without control for control systems I and II. It can be seen that both of the given control systems are sufficiently effective in reducing the vibration amplitude at both the first and the second resonances. Control system I reduces the vibration amplitude by 87.8% at the first resonance and by 89.1% at the second. Control system II reduces the vibration amplitude by 92.4% at the first resonance and by 90.7% at the second. Thus, control system II is somewhat more effective than system I. However, when system II is used, two resonances instead of one appear near the beam's first and second resonant frequencies.

The results of control in experiment and in numerical simulation are given in Table 2. The gains in the first and second loops, K_{p1} and K_{p2} are given for each of the control systems, as well as the ratio of the maximum vibration amplitude of the point at the upper end of the beam with the control turned on to the resonant vibration amplitude of this point without control at the first resonance $y_1/y^{(0)}{}_1$ and at the second resonance $y_2/y^{(0)}{}_2$. As evident from the data in Table 2, the effectiveness of modal control system I in the experiment is close to its effectiveness in numerical study, and the results of system II are better than those of system I, especially for the first resonant frequency.

Conclusion

We have constructed a finite-element model of the experimental setup given in [1, 14], taking into account the piezoelectric effect. This model allowed to numerically obtain the frequency responses for different impacts on the beam and measurements of the output signal. The calculated results were sufficiently close to

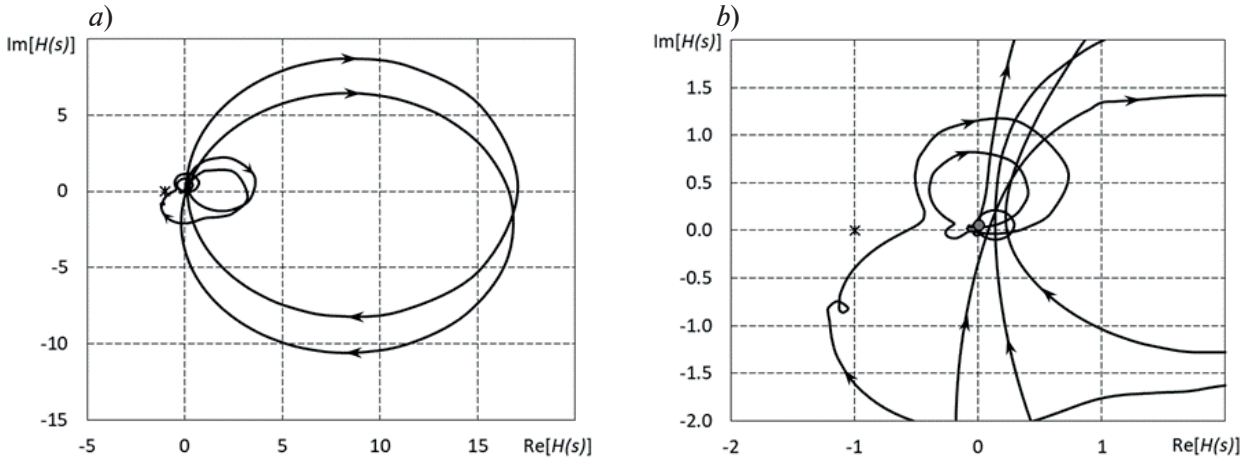

Fig. 4. Nyquist diagrams for both loops of control system I: general view (*a*) and enlarged fragment (*b*)

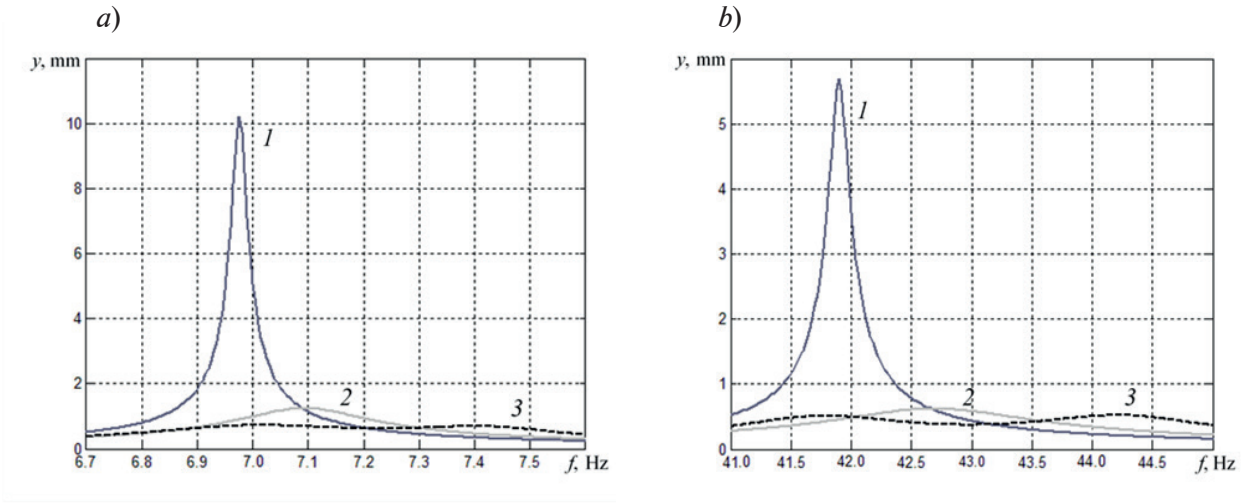

Fig. 5. Frequency response of beam without control (curve *1*) and with control for systems I (*2*) and II (*3*) near the first (*a*) and second (*b*) resonances

Table 2

Performance characteristics of different control system obtained numerically and experimentally

Control system	K_{p1}	K_{p2}	$y_1/y^{(0)}{}_1$, %	$y_2/y^{(0)}$, %
I (experiment)	0.100	0.020	16.5	12.8
I (simulation)	0.170	0.044	12.2	10.9
II (simulation)	0.530	0.650	7.6	9.3

Notations: K_{p1}, K_{p2} are the gains in the first and second loops; $y_1/y^{(0)}{}_1$, $y_2/y^{(0)}{}_2$ are the ratios of the maximum vibration amplitude of a point at the upper end of the beam with the control switched on to the resonant vibration amplitude of this point without control at the first and second resonances, respectively.

the characteristics obtained experimentally. The resonance peaks obtained by simulation and by experiment have different heights because of the difference in the damping factors of the real system and the finite element model.

Based on the frequency and phase response of the system, obtained numerically, we have constructed the solutions to the problem of beam vibrations with modal control for different control laws. The results of numerical simulation of the most effective control system created within the framework of the experiment (with resonant amplitudes at the first and second resonances decreased by 87.8% and 89.1%, respectively) proved closed to the experiment (with a decrease by 83.5% and 87.2%). We have formulated and tested more effective control laws for both loops, resulting in lower resonant amplitudes of the beam's vibrations than the systems considered in the experiment (with resonant amplitudes decreased by 92.4% and 90.7%).

Appendix

Transfer functions of control loops

Transfer function of the first loop of control system I:

$$R_1^{(1)}(s) = \left(44s^6 + 7.2\cdot10^3 s^5 + 1.3\cdot10^8 s^4 + \right.$$
$$+1.4\cdot10^{10} s^3 + 5.5\cdot10^{13} s^2 + 4.8\cdot10^{15} s +$$
$$\left.+1.1\cdot10^{17}\right)\Big/\left(s^7 + 668s^6 + 3.1\cdot10^6 s^5 + \right.$$
$$+7.4\cdot10^8 s^4 + 1.3\cdot10^{12} s^3 +$$
$$\left.+1.8\cdot10^{14} s^2 + 7.1\cdot10^{15} s + 6.3\cdot10^{17}\right).$$

Gain $K^{(1)}_{p1} = 0.170$.

Transfer function of the second loop of control system I

$$R_2^{(1)}(s) = \left(1.4\cdot10^5 s^5 + 9.3\cdot10^7 s^4 + 2\cdot10^{11} s^3 + \right.$$
$$+1.1\cdot10^{14} s^2 + 2.9\cdot10^{16} s +$$
$$\left.+1.92\cdot10^{18}\right)\Big/\left(s^7 + 1.1\cdot10^3 s^6 + 2.1\cdot10^6 s^5 + \right.$$
$$+1.8\cdot10^9 s^4 + 1.1\cdot10^{12} s^3 +$$
$$\left.+6\cdot10^{14} s^2 + 1.1\cdot10^{17} s + 4.36\cdot10^{19}\right).$$

Gain $K^{(1)}_{p2} = 0.044$.

Transfer function of the first loop of control system II:

$$R_1^{(2)}(s) = \left(403s^4 + 2.9\cdot10^4 s^3 + \right.$$
$$+9.7\cdot10^8 s^2 + 8.6\cdot10^9 s +$$
$$\left.+1.88\cdot10^{12}\right)\Big/\left(s^5 + 1.1\cdot10^3 s^4 + \right.$$
$$+2.7\cdot10^6 s^3 + 1.5\cdot10^9 s^2 +$$
$$\left.+7.8\cdot10^9 s + 3.54\cdot10^{12}\right).$$

Gain $K^{(2)}_{p1} = 0.530$.

Transfer function of the second loop of control system II:

$$R_2^{(2)}(s) = \left(2.2\cdot10^5 s^4 + 8\cdot10^6 s^3 + \right.$$
$$+2.7\cdot10^{11} s^2 + 4.2\cdot10^{12} s +$$
$$\left.+1.7\cdot10^{16}\right)\Big/\left(s^6 + 372s^5 + \right.$$
$$+1.5\cdot10^6 s^4 + 4.1\cdot10^8 s^3 +$$
$$\left.+4.2\cdot10^{11} s^2 + 3.4\cdot10^{13} s + 2.6\cdot10^{16}\right).$$

Gain $K^{(2)}_{p2} = 0.650$.

REFERENCES

[1] **A.K. Belyaev, A.V. Fedotov, H. Irschik, et al.,** Experimental study of local and modal approaches to active vibration control of elastic systems, Structural Control and Health Monitoring. 25(8) (2017) e2105.

[2] **L.A. Gould, M.A. Murray-Lasso,** On the modal control of distributed parameter systems with distributed feedback, IEEE Transactions on Automatic Control. 11(4) (1966) 729–737.

[3] **L. Meirovitch,** Dynamics and control of structures, John Wiley & Sons, New York, 1990.

[4] **C.-K. Lee, F.C. Moon,** Modal sensors/actuators, ASME Journal of Applied Mechanics. 57(2) (1990) 434–441.

[5] **A. Donoso, J.C. Bellido,** Systematic design of distributed piezoelectric modal sensors/actuators for rectangular plates by optimizing the polarization profile, Structural and Multidisciplinary Optimization. 38(4) (2009) 347–356.

[6] **U. Stoebener, L. Gaul,** Modal vibration control for PVDF coated plates, Journal of Intelligent Material Systems and Structures. 11(4) (2000) 283–293.

[7] **S. Hurlebaus, U. Stoebener, L. Gaul,** Vibration reduction of curved panels by active modal control, Computers and Structures. 86(3–5) (2008) 251–257.

[8] **G. Zenz, W. Berger, J. Gerstmayr, et al.,** Design of piezoelectric transducer arrays for

passive and active modal control of thin plates, Smart Structures and Systems. 12(5) (2013) 547–577.

[9] **F. Braghin, S. Cinquemani, F. Resta,** A new approach to the synthesis of modal control laws in active structural vibration control, Journal of Vibration and Control. 19(2) (2012) 163–182.

[10] **S. Cinquemani, D. Ferrari, I. Bayati,** Reduction of spillover effects on independent modal space control through optimal placement of sensors and actuators, Smart Materials and Structures. 24(8) (2015) 085006.

[11] **G. Canciello, A. Cavallo,** Selective modal control for vibration reduction in flexible structures, Automatica. 75 (January) (2017) 282–287.

[12] **M. Biglar, M. Gromada, F. Stachowicz, T. Trzepiecinski,** Optimal configuration of piezoelectric sensors and actuators for active vibration control of a plate using a genetic algorithm, Acta Mechanica. 226 (10) (2015) 3451–3462.

[13] **Z.-G. Song, F.-M. Li, E. Carrera, P. Hagedorn,** A new method of smart and optimal flutter control for composite laminated panels in supersonic airflow under thermal effects, Journal of Sound and Vibration. 414 (3 February) (2018) 218–232.

[14] **A.K. Belyaev, V.A. Polyanskiy, N.A. Smirnova, A.V. Fedotov,** Identification procedure in the modal control of a distributed elastic system, St. Petersburg Polytechnical University Journal: Physics and Mathematics. 10 (2) (2017) 69–81.

[15] **A. Preumont,** Mechatronics: dynamics of electromechanical and piezoelectric systems, Springer, Dordrecht, 2006.

Received 17.01.2019, accepted 18.02.2019.

THE AUTHOR

FEDOTOV Aleksandr V.
Institute for Problems in Mechanical Engineering, RAS
61 Bolshoi Ave. V.O., St. Petersburg, 199178, Russian Federation
alvafed@yandex.ru

СПИСОК ЛИТЕРАТУРЫ

1. **Belyaev A.K., Fedotov A.V., Irschik H., Nader M., Polyanskiy V.A., Smirnova N.A.** Experimental study of local and modal approaches to active vibration control of elastic systems // Structural Control and Health Monitoring. 2017. Vol. 25. No. 8. P. e2105.

2. **Gould L.A., Murray-Lasso M.A.** On the modal control of distributed parameter systems with distributed feedback // IEEE Transactions on Automatic Control. 1966. Vol. 11. No. 4. Pp. 729–737.

3. **Meirovitch L.** Dynamics and control of structures. New York: John Wiley & Sons, 1990. 425 p.

4. **Lee C.-K., Moon F.C.** Modal sensors/actuators // ASME Journal of Applied Mechanics. 1990. Vol. 57. No. 2. Pp. 434–441.

5. **Donoso A., Bellido J.C.** Systematic design of distributed piezoelectric modal sensors/actuators for rectangular plates by optimizing the polarization profile // Structural and Multidisciplinary Optimization. 2009. Vol. 38. No. 4. Pp. 347–356.

6. **Stoebener U., Gaul L.** Modal vibration control for PVDF coated plates // Journal of Intelligent Material Systems and Structures. 2000. Vol. 11. No. 4. Pp. 283–293.

7. **Hurlebaus S., Stoebener U., Gaul L.** Vibration reduction of curved panels by active modal control // Computers and Structures. 2008. Vol. 86. No. 3–5. Pp. 251–257.

8. **Zenz G., Berger W., Gerstmayr J., Nader M., Krommer M.** Design of piezoelectric transducer arrays for passive and active modal control of thin plates // Smart Structures and Systems. 2013. Vol. 12. No. 5. Pp. 547–577.

9. **Braghin F., Cinquemani S., Resta F.** A new approach to the synthesis of modal control laws in active structural vibration control // Journal of Vibration and Control. 2012. Vol. 19. No. 2. Pp. 163–182.

10. **Cinquemani S., Ferrari D., Bayati I.** Reduction of spillover effects on independent modal space control through optimal placement of sensors and actuators // Smart Materials and Structures. 2015. Vol. 24. No. 8. P. 085006.

11. **Canciello G., Cavallo A.** Selective modal control for vibration reduction in flexible structures // Automatica. 2017. Vol. 75. January. Pp. 282–287.

12. **Biglar M., Gromada M., Stachowicz F.,**

Trzepiecinski T. Optimal configuration of piezoelectric sensors and actuators for active vibration control of a plate using a genetic algorithm // Acta Mechanica. 2015. Vol. 226. No. 10. Pp. 3451–3462.

13. **Song Z.-G., Li F.-M., Carrera E., Hagedorn P.** A new method of smart and optimal flutter control for composite laminated panels in supersonic airflow under thermal effects // Journal of Sound and Vibration. 2018. Vol. 414. 3 Febrary. Pp. 218–232.

14. Беляев А.К., **Полянский В.А., Смирнова Н.А., Федотов А.В.** Процедура идентификации при модальном управлении распределенным упругим объектом // Научно-технические ведомости СПБГПУ. Физико-математические науки. 2017. Т. 10. № 2. С. 69–81.

15. **Preumont A.** Mechatronics: dynamics of electromechanical and piezoelectric systems. Dordrecht: Springer, 2006.

Статья поступила в редакцию 17.01.2019, принята к публикации 18.02.2019.

СВЕДЕНИЯ ОБ АВТОРЕ

ФЕДОТОВ Александр Васильевич – младший научный сотрудник Института проблем машиноведения РАН.

199178, Российская Федерация, г. Санкт-Петербург, Большой проспект В.О., 61.

alvafed@yandex.ru